

Supporting Information

Localised polymerisation of acrylamide using single-barrel scanning electrochemical cell microscopy

Mahir Mohammed, Bryn A. Jones, Evelina Liarou and Paul Wilson*

University of Warwick, Department of Chemistry, Library Road, Coventry, UK.

*E-mail: p.wilson.1@warwick.ac.uk

1. Experimental

1.1 – Substrate Fabrication and Chemical Solutions

Materials: Copper(II) trifluoromethanesulfonate ($\text{Cu}^{\text{II}}(\text{OTf})_2$, Acros Organics, 98%), tris(2-pyridylmethyl)amine (TPMA, Sigma Aldrich, 98%), potassium nitrate (KNO_3 , Acros Organic, 99%), Acrylamide (Am, Sigma Aldrich, 99%) were used as received without further purification. All solutions were prepared using deionised water (15.6 M Ω , VEOLIA Elga Purelab). 2-hydroxyethyl 2-bromoisobutyrate (HEBiB) was synthesised according to literature procedure and obtained with high spectroscopic purity.¹ Potassium nitrate was used as background electrolyte.

Preparation of Au and SAM/Au Electrodes: The alkanethiol, bis[2-(2-bromoisobutyryloxy)ethyl] disulphide, was synthesised according to literature.² Au substrates were prepared by sputter-coating glass microscope slides (2 mm thickness) with titanium (400 nm thickness), followed by gold (50 nm thickness). The resulting gold surface was then cleaned using acetone and then sonicated in ethanol. Before SAM experiments, the Au substrate was immersed for 36 hours in an IPA solution containing 20 mM Bis[2-(2-bromoisobutyryloxy)ethyl] disulphide to form the self-assembled monolayer (SAM). After that, the substrate was rinsed with ethanol to remove any excess alkanethiol. For all experiments, the gold substrates (with/without SAM) were glued onto Agar Scientific AFM stainless steel metal specimen discs (20 mm diameter) using Rimmel London super gel nail polish, and were connected to insulated copper wire (0.3 mm) using conductive silver epoxy

and a layer of Araldite glue was applied. They were then left to dry overnight before use the next day.

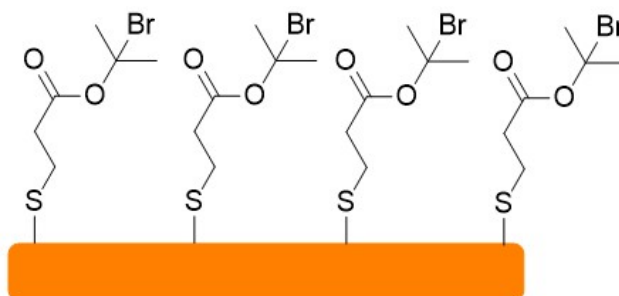


Fig S1 - showing the SAM on the gold surface when formed.

Scanning Electrochemical Cell Microscopy (SECCM) Solutions: 6.9 mM $\text{Cu}(\text{OTf})_2$, 8.63 mM TPMA, and 2.3 M (10 wt. %) acrylamide (Am), deionised water, 0.23 M HeBiB (target DP = 10) was used for SECCM polymer deposition experiments, 20 mM KNO_3 for controls using KNO_3 , with HeBiB not included where stated for control experiments.

Non-SAM Experiments: Milli-Q water (Millipore Corp) were used for SECCM. Probes. Dual barrel borosilicate glass theta pipettes (o.d. 1.5 mm, i.d. 0.23 mm, Harvard Apparatus) were pulled using a laser puller (Model P-2000, Sutter Instruments) to produce tapered pipets of either 1 μm diameter (for spot deposition) or 200 nm diameter (for dual-barrel patterning), using the details described in section 3. Pipette dimensions were acquired using field emission-scanning electron microscopy (FE-SEM Zeiss SUPRA 55VP).

Au and Au/SAM substrates within the SECCM setup were connected to a custom electrometer head (100 pA – 100 fA sensitivity) to measure surface currents.

2. Scanning Electrochemical Cell Microscopy (SECCM) Probe Fabrication and SECCM Setup

2.1 Nanopipette Fabrication (Single Barrel)

1000 nm diameter single barrel nanopipettes were pulled using borosilicate glass capillaries (o.d. 1.2 mm, i.d. 0.69 mm, Harvard Apparatus) through the use of a laser puller (P-2000, Sutter Instruments; pulling parameters: Line 1: Heat 350, Fil 4, Vel 40, Del 200, Pul 0. The inner diameter of the probe was measured using a Zeiss Supra Scanning Electron Microscopy (SEM) and using these conditions was found to consistently be 1000 nm \pm 10%. Ag/AgCl QRCEs

were used and placed in the nanopipette barrels as required, fabricated by electrolyzing silver wire in saturated potassium chloride solution.

2.2 - SECCM - Single Barrel Setup

The basic instrumentation setup is similar to that used by the Unwin group and was built following specifications provided by them. The nanopipette probes were mounted on a mechanical micro-positioner (Newport, M-461-XYZ-M) for coarse probe positioning over a surface. The fine horizontal movement of the probe was controlled using a two-axis piezoelectric positioning system with a range of 100 μm (Physik Instrumente, model P-621.2CD), while vertical movement was controlled using a single axis piezoelectric positioning stage of range 38 μm (P-753-3CD, Physik Instrumente). Coarse vertical movement was controlled using a pico motor (Newton). The piezoelectric positioners were mounted inside the Faraday cage which utilized acoustic insulation, vacuum insulating panels (Kevothermal) and aluminum heat sinks (aimed to reduce thermal fluctuations and drift of the piezoelectric positioners.) All equipment is bolted securely to a breadboard (Newport) and mounted on a vibration isolation platform (Minus K) all incorporated within the Faraday cage. The electrometer and current-voltage converter used were bespoke, both made in-house, while user control of probe position, voltage output, and data collection was *via* custom-made programs in LabVIEW (2019, National Instruments) through a field programmable graphics array (FPGA) card (7852R, National Instruments). Raw data from the instrument was processed using MATLAB (2020 version.) Deposition experiments were performed inside a Faraday cage, see figure below. The Au or Au/SAM working electrode was mounted on a high precision 100 μm range x,y- piezoelectric stage (Physik Instrumente, model P-621.2CD) and connected to a custom built electrometer (an in-house built instrument developed by Dr Alex Colburn) for surface current (i_{surface}) measurements. Single-barrel probes were used, and Ag/AgCl (Sigma Aldrich 99.99% pure Ag wire 0.125 mm diameter in 100 m reels) quasi reference counter electrodes (QRCEs) were inserted into single-barrel probes. The probe was then mounted on a high-dynamic 38 μm range z-piezoelectric positioner (P-753CD LISA, PhysikInstrumente, Germany) see figure below. The pipette was delivered to the surface as detailed in section 3 below.

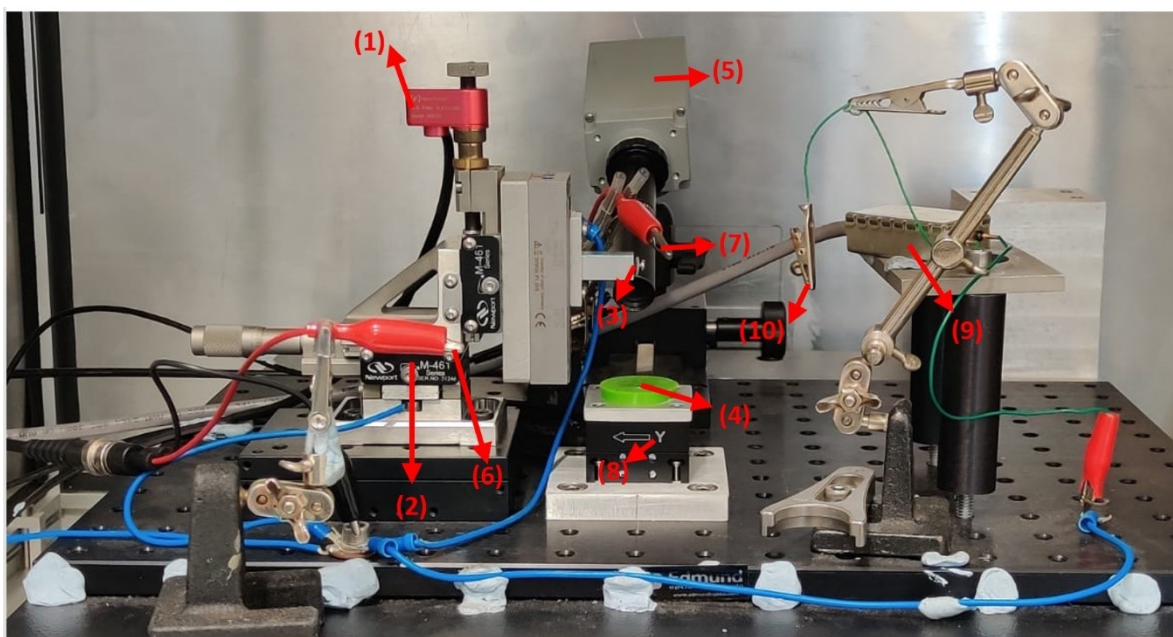


Fig S2. Photograph taken with a OnePlus 7T smartphone camera showing the SECCM microscope arrangement used. (1) z-picomotor; (2) x,y-manual stage; (3) pipette holder; (4) substrate stage, where the gold/AFM disc substrates are stucked down; (5) Pixel-Link camera used to find the nanopipette opening once the pipette is mounted on the pipette holder, used to help deliver the pipette to the substrate; (6) crocodile clip which attaches QRCE 1 (one QRCE for single barrel mode, two for dual-barrel mode); (7) crocodile clip which attaches QRCE 2; (8) x-y piezoelectric positioner; (9) electrometer head for surface current measurements; (10) crocodile clip which attaches the electrometer head to the copper wire that had been glued to the gold substrate.

3 - Carrying out a Single-Barrel SECCM Measurement

Ag/AgCl quasi reference counter electrode (QRCEs) was inserted into the barrel of the pipette, with a potential difference applied to the gold substrate, V_{surf} , depending on the experiment, and as stated in the manuscript (some value between -0.05V and -0.5V). The probe was brought close to the surface with the micro-positioner, and with the help of a camera (Pixel link with Edmund Optics lens, 6.0x magnification, 65 mm focal length) and a light box. The SECCM probe was moved vertically towards the biased gold WE surface using the z-piezo via the 'Approach and CV' (cyclic voltammetry) or 'Approach and IT' (constant potential) program, using a surface current threshold of -10 pA to detect when the meniscus had made contact with the surface and halt further approach when this threshold had been met. Slow

approach speeds of 1 μm per second were used to prevent tip crashing. Note that the probe itself never makes contact with the WE surface. Electrochemical measurements were performed in the localized area defined by the meniscus cell formed between the SECCM probe tip and WE surface. Cyclic voltammetry was carried out using a fixed potential window (-0.6 V to 0.4 V) and fixed scan rate (0.1 vps), whilst constant potential experiments used a particular V_{surf} value depending on the experiment. If we assume the probe was 10 μm above the surface before making contact, the probe would then move automatically back to that position in the z-axis (or whatever height it was before the approach and CV/IT program was executed), guided by the piezoelectric positioners. In the LabVIEW program used, the probe would then be programmed by manual user input to move (for example) 40 μm in the y-axis to the next position (see diagram), and the probe would then execute another approach and CV/IT procedure as outlined. The surface is biased (V_{surf}) and the current (I_{surf}) is measured at the Ag/AgCl QRCE as schematically shown below (Fig. S3). The components of the solution used in our nanopipette are as described in section 1.

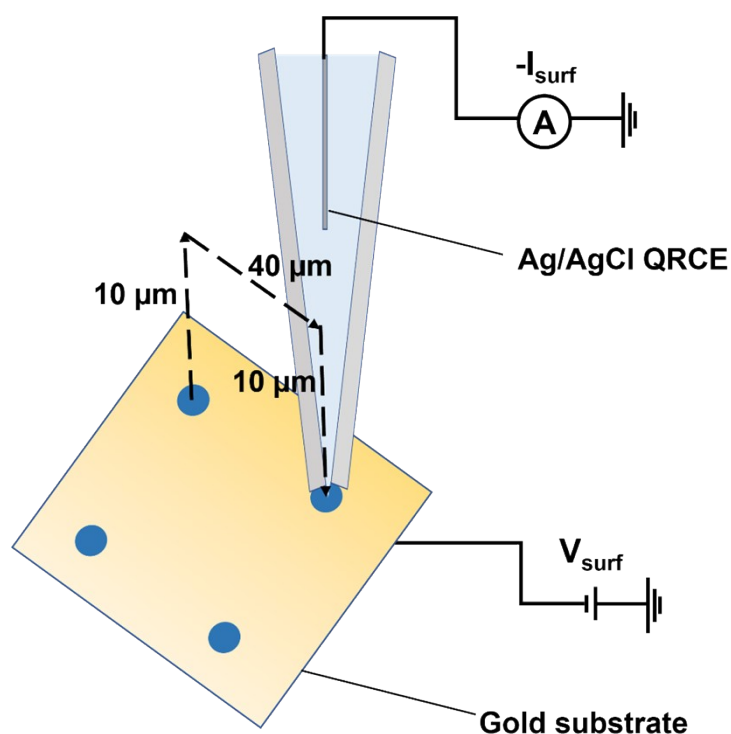


Fig S3. Schematic of the single-barrel SECCM arrangement used for cyclic voltammetry and constant potential measurements used in this paper, showing the V_{surf} and I_{surf} parameters and how they are applied.

4 – Scanning Electron Microscopy

Nanopipette images were taken using a Zeiss Supra 55VP SEM instrument, with a working distance of 6.1 mm, and an EHT of 5 kV. A Zeiss Gemini 500 Field Emission instrument was used to take images of the polymeric gels, using a weak EHT of 0.5 kV (lower voltages are enabled by the Gemini device) to prevent damage to the soft polymer gels, and a working distance of 3.3 mm.

5 – Atomic Force Microscopy

Atomic force microscopy images were taken using a Bruker-Nano Enviroscope AFM using the SCANASYST regime which monitors image quality and makes automatic parameter adjustments, using a scan rate of 0.1 microns per second and a SCANASYST-Air Bruker AFM tip.

6. Supporting Figures

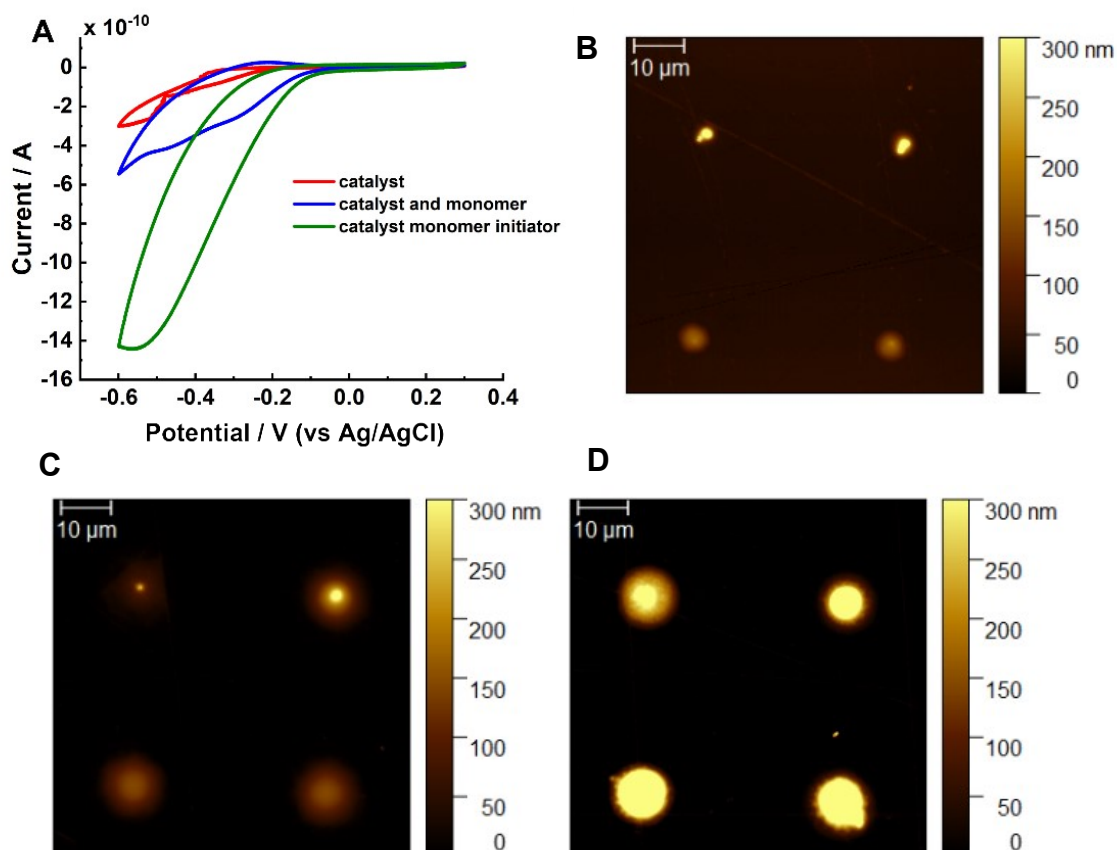


Fig S4. (A) Cyclic voltammetry (CV) of (red) 6.9 mM Cu^{II}TPMA in H₂O; (blue) 6.9 mM Cu^{II}TPMA and 10 wt% Am in H₂O; (green) 6.9 mM Cu^{II}TPMA, 10 wt% Am, and 0.23 M HeBiB in H₂O. Scan rate : 0.1 vps. AFM analysis of the landing sites arising from the CV of (B) 6.9 mM Cu^{II}TPMA in H₂O; (C) 6.9 mM Cu^{II}TPMA and 10 wt% Am in H₂O; (D) 6.9 mM Cu^{II}TPMA, 10 wt% Am, and 0.23 M HeBiB in H₂O. Scan rate : 0.1 vps.

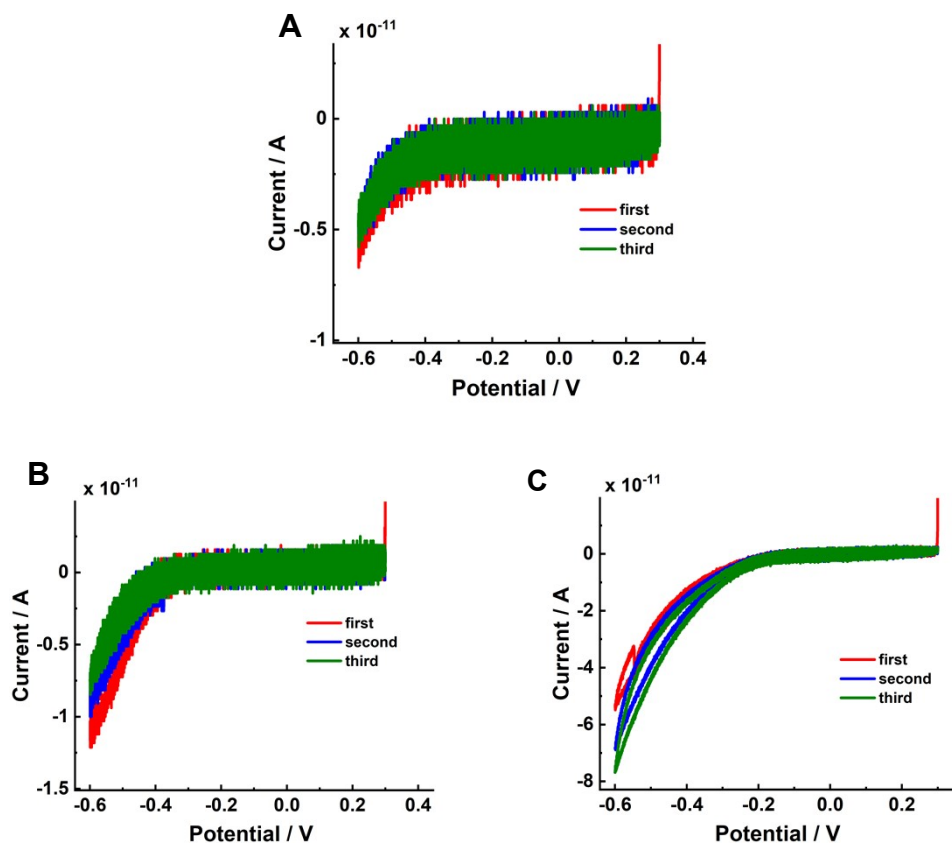


Fig S5. Cyclic voltammetry of (A) 20 mM KNO₃ in H₂O; (B) 20 mM KNO₃ and 10 wt% Am in H₂O; (C) 20 mM KNO₃, 10 wt% Am, and 0.23 M HeBiB in H₂O. Scan rate: 0.1 vps.

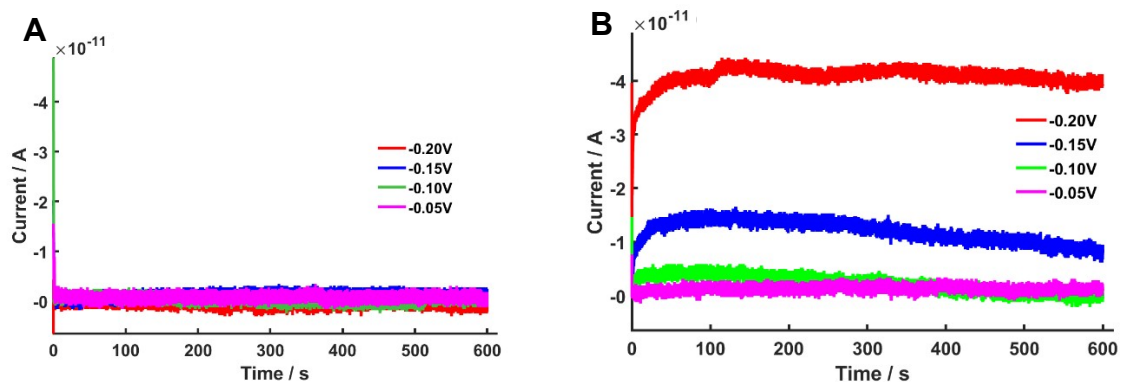
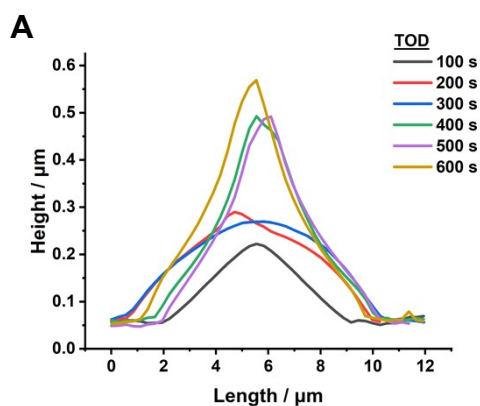


Fig S6. (A) i vs t recorded after the potentiostatic ($V_{\text{surf}} = -0.05$ V, $V_{\text{surf}} = -0.10$ V, $V_{\text{surf}} = -0.15$ V, $V_{\text{surf}} = -0.20$ V) single-barrel SECCM deposition of KNO_3 , monomer and initiator using $[\text{Am}] : [\text{HEBiB}] = [20] : [1]$, 10 wt % Am and in the presence of 20 mM KNO_3 at room temperature. (B) i vs t recorded after depositions observed when performing the potentiostatic ($V_{\text{surf}} = -0.05$ V, $V_{\text{surf}} = -0.10$ V, $V_{\text{surf}} = -0.15$ V, $V_{\text{surf}} = -0.20$ V) single-barrel SECCM eATRP of Am using $[\text{Am}] : [\text{HEBiB}] : [\text{Cu}^{\text{II}}] : [\text{TPMA}] = [20] : [1] : [0.5] : [0.625]$ at room temperature.



B

C

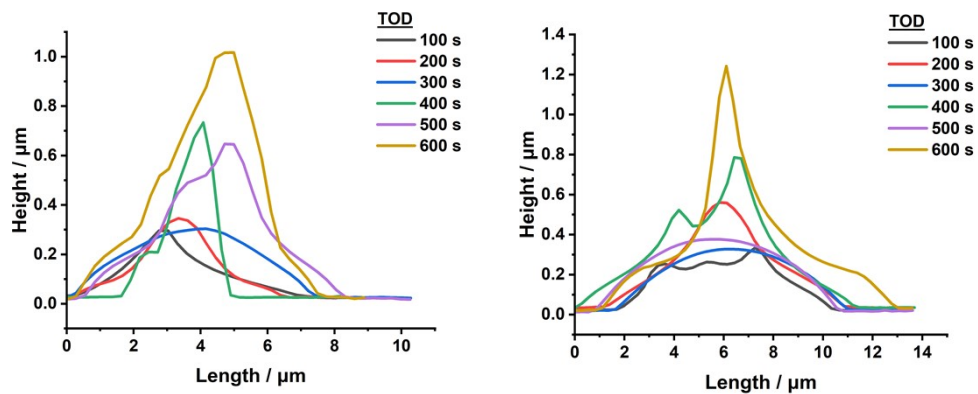


Fig S7. (A), (B) and (C) are line-profiles of the cross-section of each AFM image of the potentiostatic ($V_{surf} = -0.15$ V) single-barrel SECCM eATRP of Am using [Am] : [HEBiB] : [Cu^{II}] : [TPMA] = [20] : [1] : [0.5] : [0.625] at room temperature, at different times of deposition (100 s, 200 s, 300 s, 400 s, 500 s, 600 s).

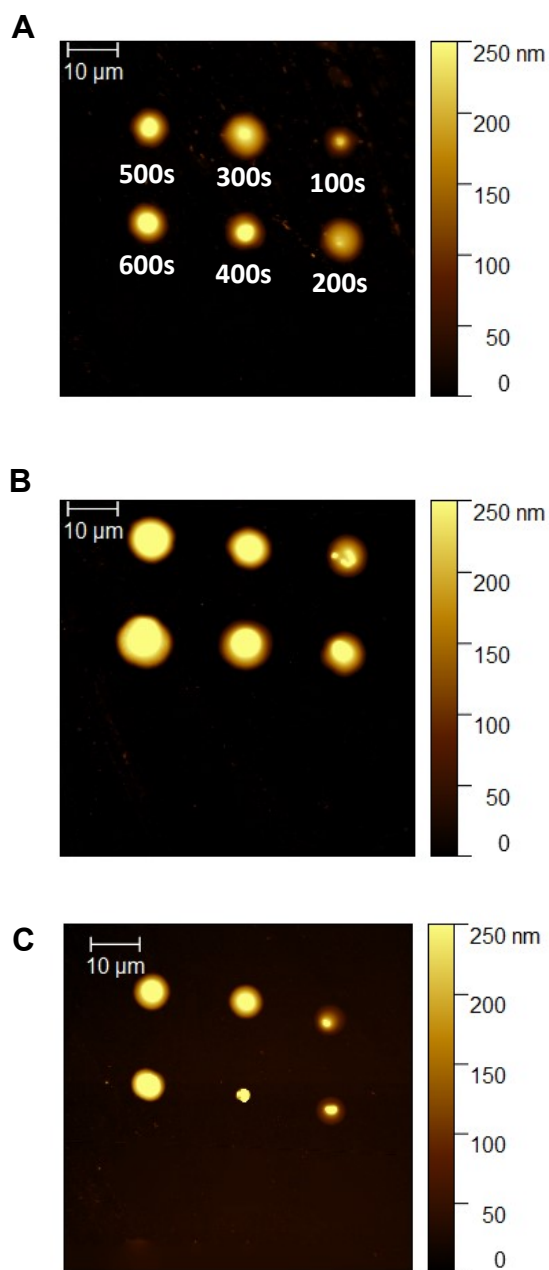


Fig S8. (A), (B) and (C) are AFM images of the potentiostatic ($V_{\text{surf}} = -0.15 \text{ V}$) single-barrel SECCM eATRP of Am using $[\text{Am}] : [\text{HEBiB}] : [\text{Cu}^{\text{II}}] : [\text{TPMA}] = [20] : [1] : [0.5] : [0.625]$ at room temperature, at different times of deposition (100 s, 200 s, 300 s, 400 s, 500 s, 600 s).

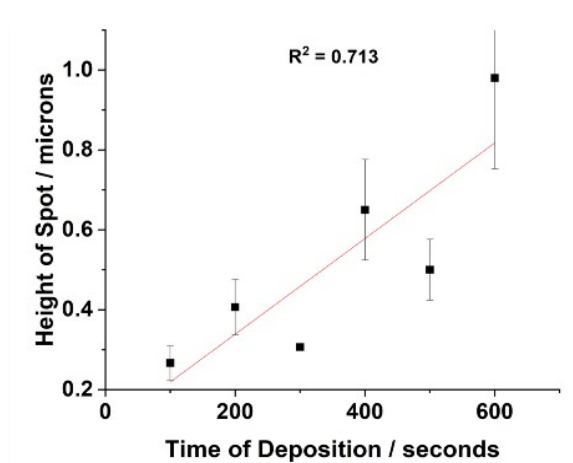


Fig. S9 Average height as a function of TOD for PAm features prepared by single-barrel SECCM eATRP of Am using [Am] : [HEBiB] : [Cu^{II}] : [TPMA] = [20] : [1] : [0.5] : [0.625] at room temperature.

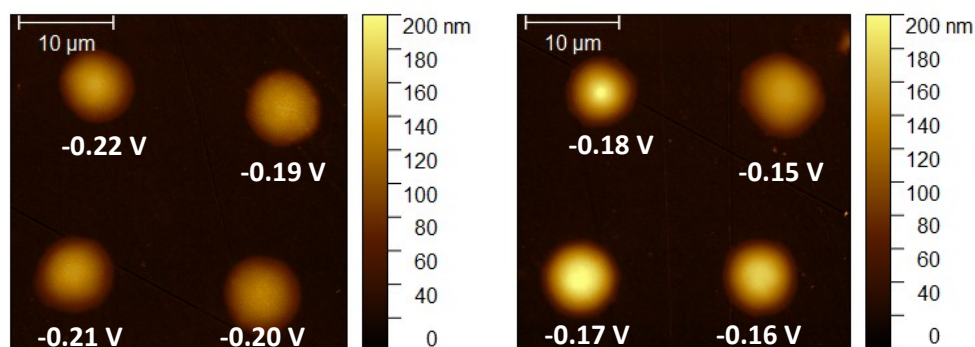


Fig S10. AFM images of the depositions produced during potentiostatic ($V_{\text{surf}} = -0.15 \text{ V}$, $V_{\text{surf}} = -0.16 \text{ V}$, $V_{\text{surf}} = -0.17 \text{ V}$, $V_{\text{surf}} = -0.18 \text{ V}$, $V_{\text{surf}} = -0.19 \text{ V}$, $V_{\text{surf}} = -0.20 \text{ V}$, $V_{\text{surf}} = -0.21 \text{ V}$, $V_{\text{surf}} = -0.22 \text{ V}$) single-barrel SECCM eATRP of Am using [Am] : [HEBiB] : [Cu^{II}] : [TPMA] = [20] : [1] : [0.5] : [0.625] at room temperature with deposition time 200 seconds.

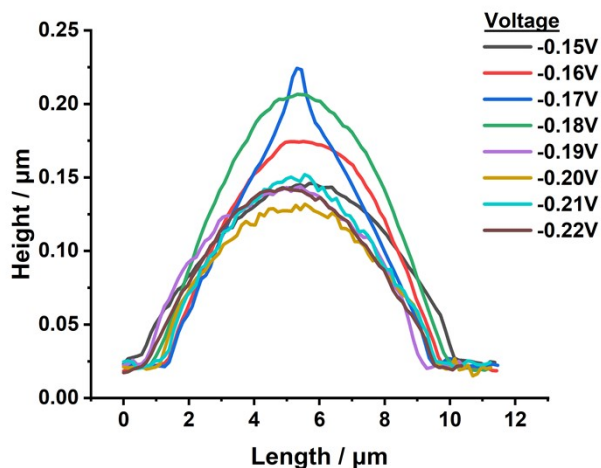


Fig S11. AFM images of the depositions produced during potentiostatic ($V_{\text{surf}} = -0.15 \text{ V}$, $V_{\text{surf}} = -0.16 \text{ V}$, $V_{\text{surf}} = -0.17 \text{ V}$, $V_{\text{surf}} = -0.18 \text{ V}$, $V_{\text{surf}} = -0.19 \text{ V}$, $V_{\text{surf}} = -0.20 \text{ V}$, $V_{\text{surf}} = -0.21 \text{ V}$, $V_{\text{surf}} = -0.22 \text{ V}$) single-barrel SECCM eATRP of Am using $[\text{Am}] : [\text{HEBiB}] : [\text{Cu}^{\text{II}}] : [\text{TPMA}] = [20] : [1] : [0.5] : [0.625]$ at room temperature, with deposition time 200 seconds.

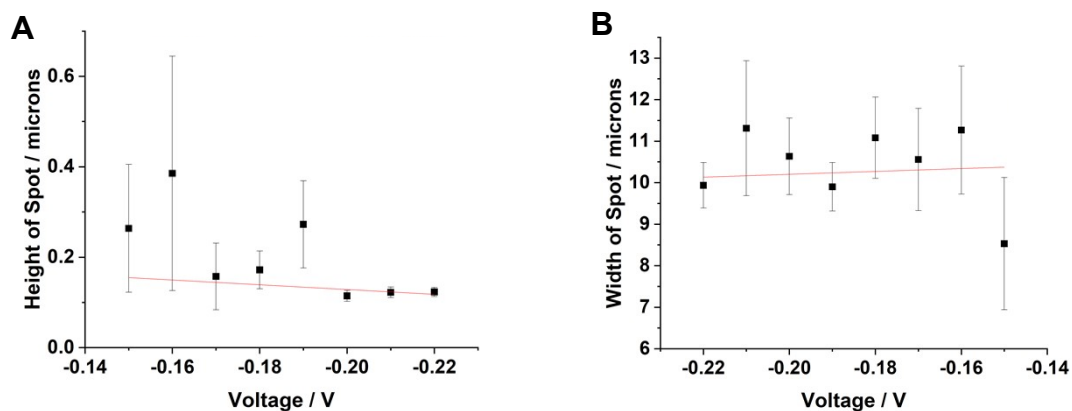


Fig S12. (A) – the mean height of each spot from Fig S9 and S10 deposited versus the voltage, V_{surf} . (B) – the mean width of each spot from Fig S9 and S10 versus the time of deposition.

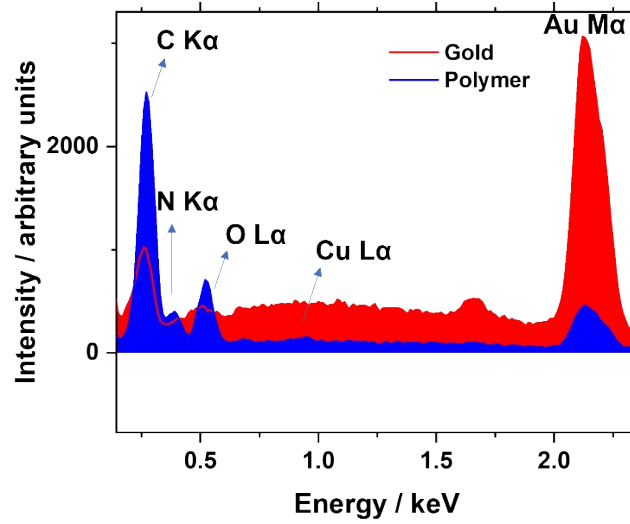


Fig S13. SEM EDX of PAM spot deposited during an 1800 second deposition ($V_{\text{surf}} = -0.15 \text{ V}$) utilizing single-barrel SECCM eATRP of Am using $[\text{Am}] : [\text{HEBiB}] : [\text{Cu}^{\text{II}}] : [\text{TPMA}] = [20] : [1] : [0.5] : [0.625]$ at room temperature.

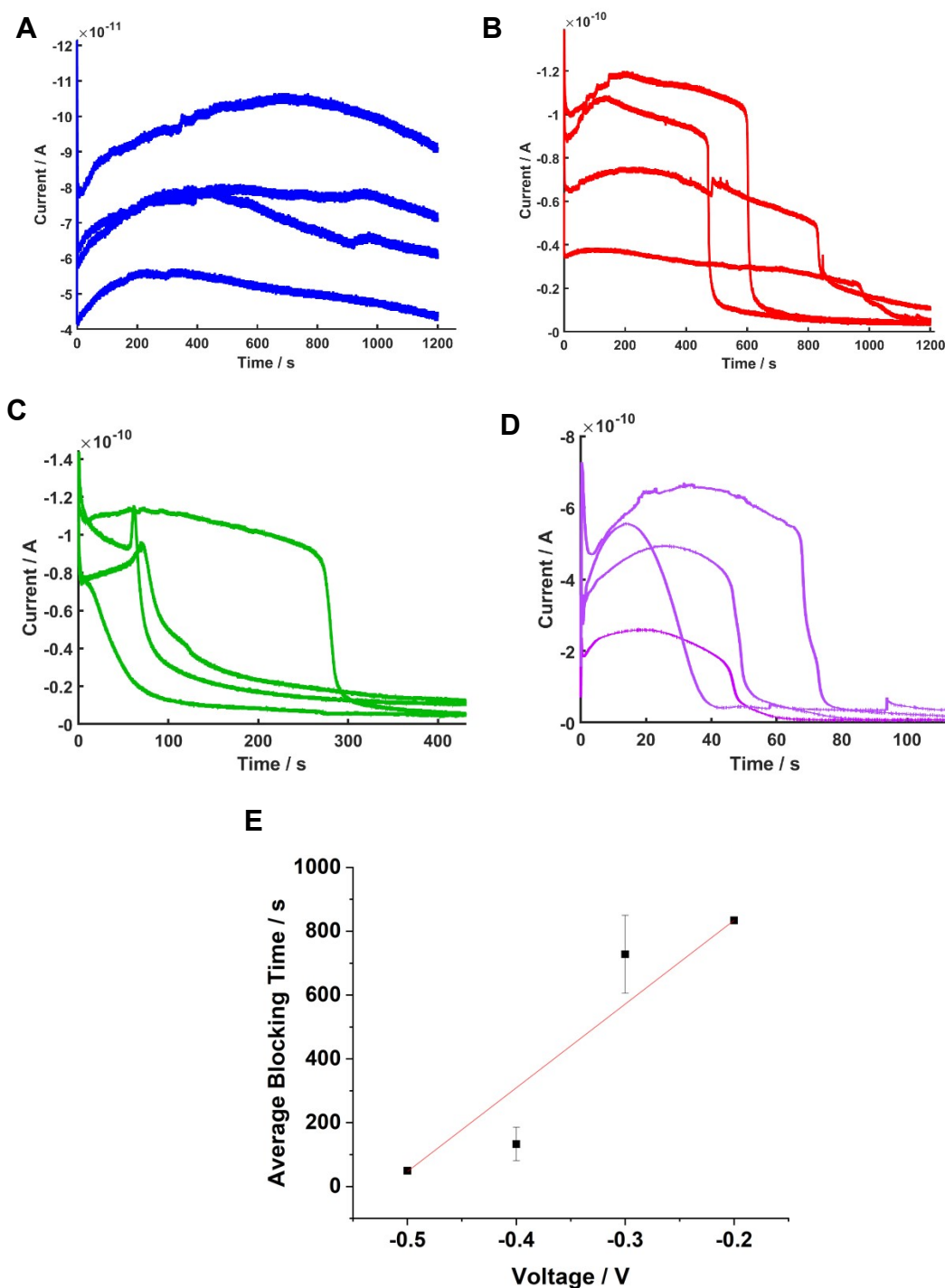


Fig S14. Current vs time plots recorded during the potentiostatic ($V_{\text{surf}} = -0.20$ V (A), $V_{\text{surf}} = -0.30$ V (B), $V_{\text{surf}} = -0.40$ V (C), $V_{\text{surf}} = -0.50$ V (D)) single-barrel SECCM eATRP of Am using [Am] : [HEBiB] : [Cu^{II}] : [TPMA] = [20] : [1] : [0.5] : [0.625] at room temperature. (E) Plot of the average blocking time versus the voltage applied, showing the strong linear correlation between blocking time and voltage applied.

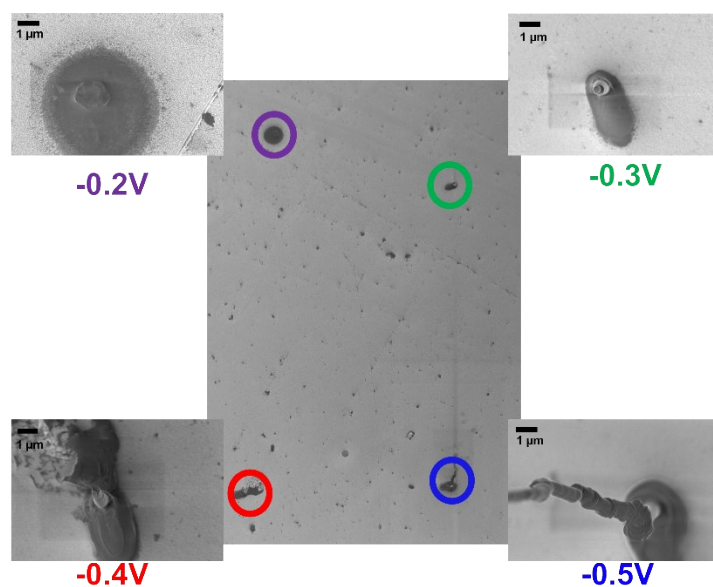


Figure S15. SEM image of the spots deposited via the potentiostatic ($V_{\text{surf}} = -0.20$ V (top left), $V_{\text{surf}} = -0.30$ V (top right), $V_{\text{surf}} = -0.40$ V (bottom left), $V_{\text{surf}} = -0.50$ V (bottom right)) single-barrel SECCM eATRP/FRP of Am using $[\text{Am}] : [\text{HEBiB}] : [\text{Cu}^{\text{II}}] : [\text{TPMA}] = [20] : [1] : [0.5] : [0.625]$ at room temperature.

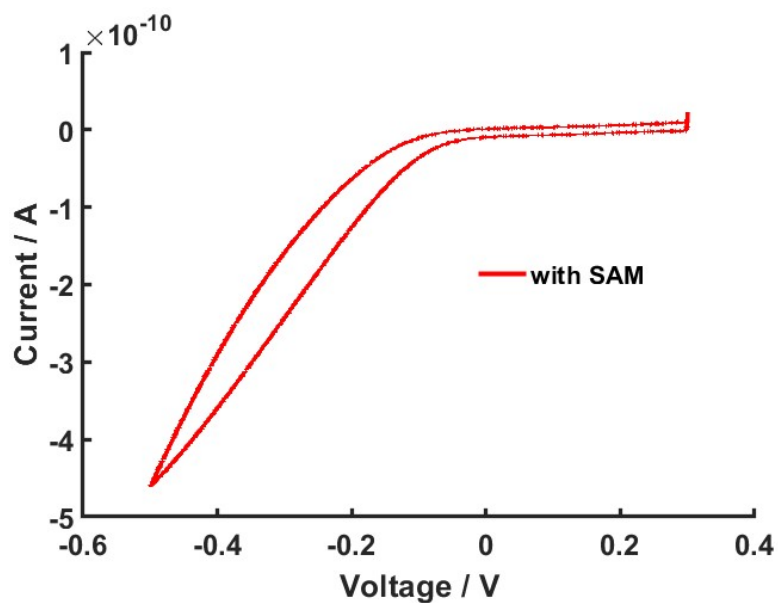


Fig S16. Cyclic voltammetry showing the effect of SAM-functionalised electrode surface. 6.9 mM $\text{Cu}^{\text{II}}\text{TPMA}$ and 10 wt% Am in H_2O .

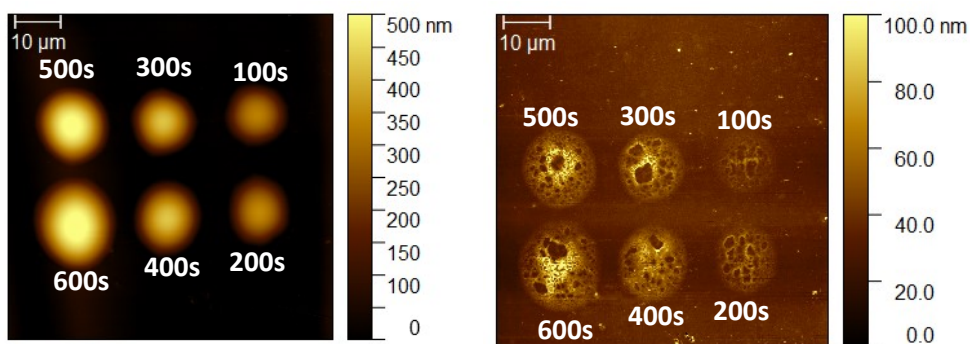


Fig S17. AFM images of the features deposited by potentiostatic ($V_{\text{surf}} = -0.15$ V) single-barrel SECCM eATRP of Am using $[\text{Am}] : [\text{Cu}^{\text{II}}] : [\text{TPMA}] = [20] : [0.5] : [0.625]$ at room temperature, with a SAM-functionalised gold substrate, at different times of deposition (100 s, 200 s, 300 s, 400 s, 500 s, 600 s). Left image shows features before rinsing with distilled water. Right image shows the corresponding features after rinsing with distilled water.

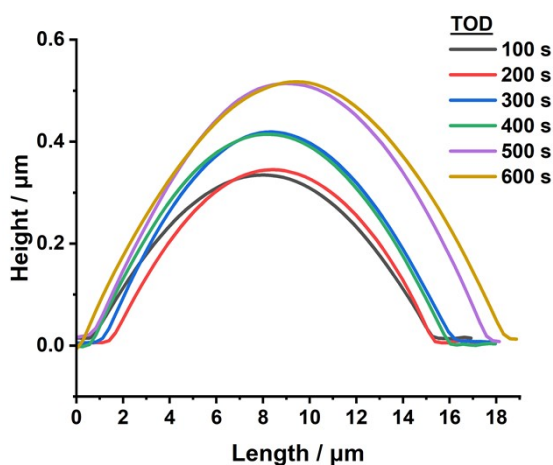


Fig S18. Line-profiles of the cross-section of each AFM image of the features deposited via potentiostatic ($V_{\text{surf}} = -0.15$ V) single-barrel SECCM eATRP of Am using $[\text{Am}] : [\text{Cu}^{\text{II}}] : [\text{TPMA}] = [20] : [0.5] : [0.625]$ at room temperature, with SAM utilized, at different times of deposition (100 s, 200 s, 300 s, 400 s, 500 s, 600 s), before rinsing.

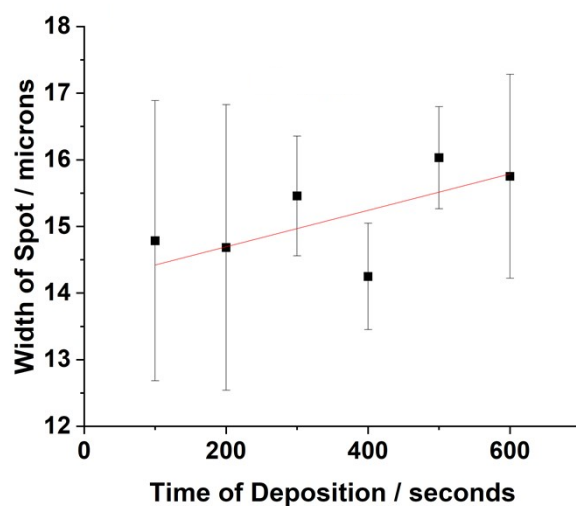


Fig S19. The mean width of each spot, before rinsing, from figures S16A, S16C, S16E and S17 versus the time of deposition.

¹ S. E. Edwards, S. Flynn, J. J. Hobson, P. Chambon, H. Cauldbeck and S. P. Rannard, *RSC Advances*, 2020, **10**, 30463-30475.

² J. P. Collman, N. K. Devaraj, T. P. A. Eberspacher and C. E. D. Chidsey, *Langmuir*, 2006, **22**, 2457–2464.